Comparative Studies on Water- and Vapor-Based Hydrothermal Carbonization: Process Analysis

Kyoung S. Ro [1],*, **Judy A. Libra** [2],* and **Andrés Alvarez-Murillo** [3]

[1] USDA-ARS Coastal Plains Soil, Water & Plant Research Center, Florence, SC 29501, USA
[2] Leibniz Institute for Agricultural Engineering and Bioeconomy, 14469 Potsdam, Germany
[3] Department of Applied Physics, School of Industrial Engineering, University of Extremadura, 06006 Badajoz, Spain; andalvarez@unex.es
* Correspondence: kyoung.ro@usda.gov (K.S.R.); jlibra@atb-potsdam.de (J.A.L.); Tel.: +1-843-669-5203 (K.S.R.); +49-331-5699-866 (J.A.L.)

Abstract: Hydrothermal carbonization (HTC) reactor systems used to convert wet organic wastes into value-added hydrochar are generally classified in the literature as liquid water-based (HTC) or vapor-based (VTC). However, the distinction between the two is often ambiguous. In this paper, we present a methodological approach to analyze process conditions for hydrothermal systems. First, we theoretically developed models for predicting reactor pressure, volume fraction of liquid water and water distribution between phases as a function of temperature. The reactor pressure model predicted the measured pressure reasonably well. We also demonstrated the importance of predicting the condition at which the reactor system enters the subcooled compression liquid region to avoid the danger of explosion. To help understand water–feedstock interactions, we defined a new solid content parameter $\%S(T)$ based on the liquid water in physical contact with feedstock, which changes with temperature due to changes in the water distribution. Using these models, we then compared the process conditions of seven different HTC/VTC cases reported in the literature. This study illustrates that a large range of conditions need to be considered before applying the label VTC or HTC. These tools can help in designing experiments to compare systems and understand results in future HTC research.

Keywords: hydrothermal carbonization (HTC); vapothermal carbonization (VTC); reactor pressure; process conditions; phase distribution of water; solid contents; hydrochar

1. Introduction

The process of hydrothermal carbonization (HTC) is used to carbonize organic residues and wastes for diverse applications ranging from fuels to soil amendments. In HTC, subcritical water is used as a solvent and reactant to transform a wide variety of organic feedstocks to solid carbonaceous products (hydrochar), which usually contain higher carbon contents, heating values and degrees of aromaticity than the original feedstocks [1–4]. Diverse types of reactors have been used, ranging from batch [3,5–12], semi-batch [2,9,10] to continuous reactors [13], with and without mixing, using direct heating through steam injection or through the reactor walls with controlled heating rates, or indirectly in muffle ovens. The pressurized reaction system usually consists of all three phases (gas, liquid, solid) and is heated to temperatures from 160 to 280 °C with pressures between 0.6 and 6.4 MPa due to the water vapor and gases produced in the reactions. Water is initially introduced into the reaction system via the moisture content of the feedstock and/or through the addition of water as a liquid or as steam. Common HTC process variations are differentiated according to how the water initially contacts the feedstock. When the feedstock is immersed in bulk liquid water, it is often called HTC.

Where the feedstock is in direct contact with only steam, it is often called steam HTC, vapor HTC or vapothermal carbonization (VTC) [2,7,10,11]. Here, feedstock can be held in baskets away from liquid water, transported in and out on conveyor belts with little to no post-processing dewatering steps necessary. However, the dividing line between the two process types often does not remain sharp over the operating time, since the distribution of water between the liquid and vapor phases will change as temperature rises in batch systems, or as more steam is added in semi-batch systems. Usually we cannot see inside high-pressure reaction systems to gain visual insights, so the extent of the phase change is often unknown. Process comparisons between HTC vs. VTC based on the state of the initial water phase may be misleading. The phase changes may play an important role in causing structural variations in the hydrochars produced, their biodegradability, stability, and functionality in various applications [5].

Only a few studies comparing hydrochars produced by HTC vs. VTC have been reported in the literature. Cao et al. [5] found that biomass was more carbonized under liquid water in HTC than through steam in VTC. They determined that more aromatic and less alkyl groups were formed in the sugar beet and bark hydrochars made from HTC than in those from VTC under the same operating conditions (200 °C for 3 h). The hydrochars made from HTC also were less biodegradable than those from VTC as indicated by the lower values of the ratio BOD/COD for HTC-hydrochars. The lower biodegradability of hydrochar from HTC was probably due to its higher aromaticity produced during the reactions taking place in liquid water. In this case, the hydrochar made from HTC should be more stable in the environment than that made from VTC, which would have consequences for its use, e.g., as a soil amendment. On the other hand, comparisons between hydrochars from HTC vs. VTC for use as fuels have produced mixed results on how the phase of the reaction medium affects the important energy parameters: solid yield, higher heating value (HHV) and energy yield [10,11,14]. Comparing HTC vs. VTC for two feedstocks, digestate and straw, at 230 °C, 6 h, Funke et al. [11] found no clear trend in HHV: VTC-chars had a higher HHV than HTC-chars from digestate, but for straw, the order was reversed. However, VTC produced higher solid yields and, therefore, higher energy yields than HTC for both feedstocks. In contrast, Shafie et al. and Yeoh et al. reported mostly lower solid yields and higher HHV from the VTC process compared to HTC process (both at 220 °C, 1 h; two feedstocks [10,14], three feedstocks [14]). Again, as in [11], the combination of these two trends in the energy yield showed that the VTC process was more efficient for energy yield. We suspect that the reason for these conflicting trends in HHV and solid yield arise from the fact that a clear picture of how the water was distributed between gas and liquid phases was not given, nor to which extent the feedstocks were exposed to the liquid water phase. For instance, the VTC experimental setup used by Yeoh et al. (two concentric chambers with water filled in the outside chamber and the biomass in the inner chamber) was assumed to avoid the liquid water directly contacting the biomass feedstock. Yet it is not clear from their description that the liquid water was contained in the outside chamber throughout the reaction, since liquid water expands at higher temperature, possibly causing overflow into the biomass chamber. It appears that the transition between HTC/VTC reported in the literature is fuzzy at best because it can be changed by small variations in the same reactor system. How much water is present in each phase depends not only on the reactor temperature and pressure, but also on the total amount of water in the system relative to the volume of the reactor system.

As more knowledge is gained on the beneficial applications of hydrochars and HTC for waste and residue processing, more work on reactor designs for diverse settings (ranging from high to low tech systems) will be carried out. The variety of process variations may increase, with process configurations and conditions utilizing the unique transport properties of each medium, e.g., the higher thermal conductivity of bulk liquid water or the higher diffusivity of steam to penetrate the porous structure of the feedstock [7,15]. These changes in transport properties can affect reactions and product characteristics [15]. Therefore, knowledge on what influences the distribution of water between the reaction phases is essential for the production of the desired hydrochar quality. Especially if we want to replicate process conditions in various reactor types and scales to produce a desired hydrochar

quality, we must be able to predict the distribution of water between the vapor and liquid phases at the design HTC reaction conditions.

Furthermore, reactor designs must consider how the HTC reactor pressure will change in response to operating conditions to ensure process safety. All reactors must be able to withstand the high temperatures and pressures that can develop during the process. As a rigid HTC reactor partially filled with water and feedstock is heated, the increase in the saturated water vapor and gases produced by the chemical reactions cause the reactor pressure to rise. At the same time, the density of the bulk liquid water decreases and consequently the volume of liquid water increases, decreasing the volume of the reactor headspace. When the liquid volume in the HTC reactor completely fills the headspace, it can no longer expand if the reactor temperature is increased further. The reactor water then enters a subcooled liquid compression region. In this region, pressure increases very rapidly with small increases in reactor temperature. To avoid the reactor pressure exceeding the tensile strength of reactor material, it is very important that the reactor system has a working safety disk or valve that can release pressure at a preset value. Without the use of proper rupture disks, the reactor can explode. Therefore, in order to maintain safe operating conditions, we need to predict the reactor pressure at the chosen process conditions. This requires understanding the relationship between the HTC reactor conditions (temperature, water volume, feedstock) and pressure.

The aim of this work is to present a methodological approach to analyze process conditions for hydrothermal systems in the framework of the hydrothermal carbonization reactions. In the paper, we first theoretically develop models for predicting reactor pressure, the distribution of water between phases, and the liquid water volume fractions as a function of reactor temperatures. Then, the evaluation is expanded to water and feedstock. Finally, using these new models, we analyze and compare process conditions for VTC and HTC systems reported in the literature.

2. Materials and Methods

2.1. Theoretical Development

For a reactor without any HTC reaction (i.e., without any feedstock inside reactor), we can estimate the HTC autogenic pressure with that of pure water at the HTC reaction temperature. This information is often visualized for hydrothermal systems with a pressure-temperature (*P-T*) phase diagram for water, showing the regions for the different types of processes, e.g., gasification, liquefaction, carbonization. However, to help us understand the process conditions during a hydrothermal reaction, the use of the temperature-volume (*T-v*) phase diagram for water is a powerful tool which provides information on *P* and *T* as well as the distribution of water between phases as a function of the overall specific volume of water (liquid and steam) in the reactor v_R (Figure 1). Using this diagram, one can understand the thermodynamic equilibrium at the chosen process conditions of the reactor system, e.g., temperature, pressure and mass of water in the system. In Figure 1, the saturation line represents the boundary condition for the phase change. For most HTC/VTC reactor systems, the reaction zone is usually located within the saturation curve, where steam and liquid phases coexist. The operating path for a batch system can be followed from the starting process conditions until the target conditions are met and the holding time begins. The closer the target point is to the steam or liquid saturation lines, the higher the amount of that phase. Since a log scale is used for the x-axis, the ratio between the two phases cannot easily be determined visually from the figure. The calculation procedure is developed in the following section.
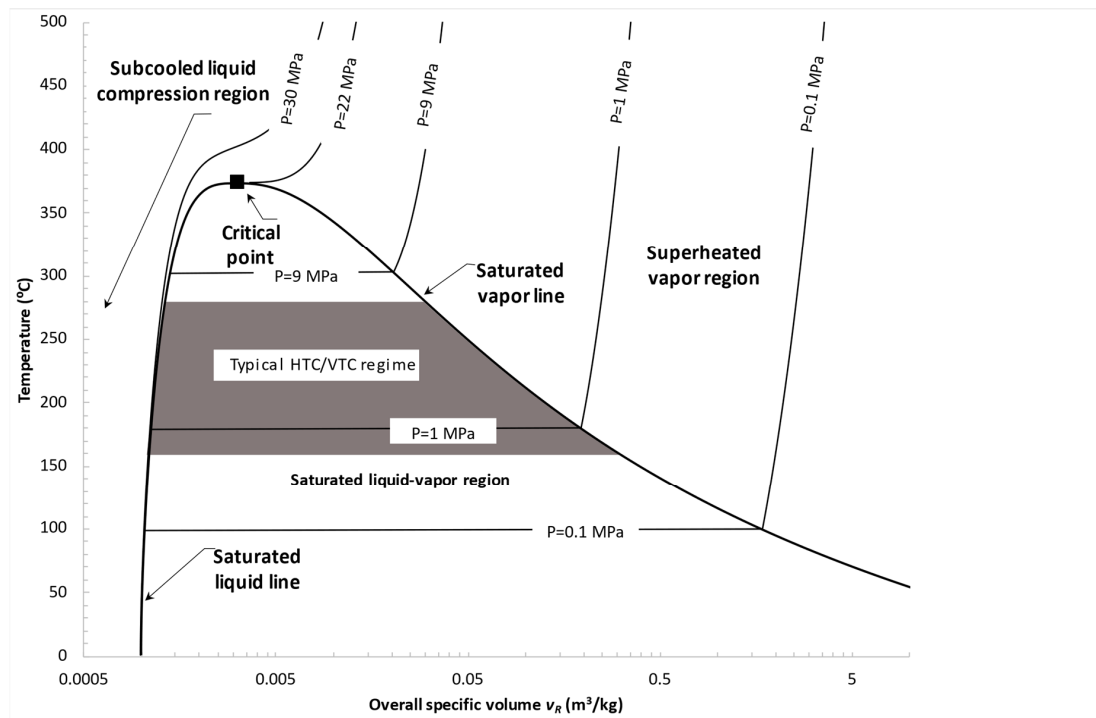
Figure 1. Temperature-volume (*T-v*) diagram for water showing the common operating region for vapor and hydrothermal carbonization reactions.

Total mass of water in the reactor is

$$M_{H2O} = x_L M_{H2O} + x_V M_{H2O} \tag{1}$$

where

M_{H2O} = total mass of liquid and vapor water in the reactor (kg);
x_L = mass fraction of liquid water;
x_V = mass fraction of vapor water (or steam quality);
$x_L + x_V = 1$.
As the HTC reactor is heated beyond the boiling temperature, the reactor volume is mostly filled with liquid water and steam, and the following relationship can be developed assuming both liquid water and steam are in equilibrium (i.e., for the saturated liquid–vapor region; Figure 1).

$$V_R = x_L M_{H2O} v_L + x_V M_{H2O} v_V \tag{2}$$

where

V_R = reactor volume (m^3);
v_L = specific volume of saturated liquid water (m^3/kg);
v_V = specific volume of saturated steam (m^3/kg).
Combining Equations (1) and (2), the mass fraction of vapor water (x_v) can be calculated by knowing the thermophysical properties of water at those conditions, the mass of water in the reactor and the reactor volume:

$$x_V = \frac{v_R - v_L}{v_V - v_L} \tag{3}$$

where

$v_R = V_R/M_{H2O}$, overall specific volume of reactor water and steam mixture (m^3/kg).
As the liquid-steam mixture in the reactor is heated, the volume of liquid water expands due to the decrease in water density ρ_L. Using Equation (3) along with values for saturated vapor and liquid

specific volumes [16], the fraction of liquid-water occupying the reactor volume VF_w can be estimated at the HTC reaction temperature:

$$VF_w = \frac{V_w}{V_R} = \frac{(1 - x_V)v_L}{v_R} \tag{4}$$

where

V_w = volume of liquid water in the reactor at temperature T (m³);

VF_w = volume fraction of liquid water in the reactor at temperature T (-).

As long as the reactor volume is larger than the bulk liquid water volume (i.e., $VF_w < 1$), we can assume the liquid and vapor water phases are in equilibrium and the autogenic pressure can be estimated from the saturation properties of water using saturated steam tables [16–18].

If the temperature is further increased so that the liquid volume completely fills the reactor due to the decrease in its density (i.e., $VF_w = 1$, and $x_L = 1$), the liquid water will enter the subcooled liquid compression region. This region can be seen in the *T-v* phase diagram, left of the saturated vapor curve (Figure 1). There is no longer any headspace in the reactor and the water density in the reactor system at this point (also called overall reactor water density) becomes constant and can be calculated from $D = M_{H2O}/V_R$. As the rigid reactor walls are suppressing the tendency of the liquid volume to increase in response to the decrease in liquid water density, the reactor pressure increases rapidly as the water expands with the increase in temperature. When $VF_w \geq 1$ calculated from Equation (4) (i.e., physically impossible unless the reactor explodes), the reactor pressure in this range can be estimated with liquid compressibility factor for subcooled water:

$$P = Z_L \times D \times RT/MW_{H2O} \tag{5}$$

where

P = reactor pressure (MPa);

Z_L = liquid compressibility factor for subcooled water (-);

D = overall reactor water density, M_{H2O}/V_R (kg/m³);

R = universal gas constant (8.31451×10^{-3} m³-MPa/kmol-K);

T = reactor temperature (K);

MW_{H2O} = molecular weight of water (kg/kmol).

To illustrate the danger of a potential reactor explosion if the liquid fills the reactor completely, example calculations to estimate the reactor pressure at three common HTC temperatures using Equation (5) are reported in Table 1. The values of liquid compressibility factor of the subcooled water reported by Lemmon et al. (2018) were used. A value for D was chosen that is slightly higher than the saturated liquid water density at 200 °C. This simulates the reactor pressure for the case when the liquid water fills the reactor completely at 200 °C. A further increase in T to 250 °C will rapidly increase P from 2 to 81.6 MPa, a pressure that many HTC reactors are not made to withstand. For instance, maximum allowable pressures for common laboratory reactors range from 13.3 to 34.5 MPa [19]. In contrast, if there is less liquid water added and more headspace in the reactor so that the liquid water-vapor equilibrium can exist at all operating temperatures, the pressure increase would follow the saturation pressure, increasing only from 1.6 to 4.0 MPa.

In order to avoid the subcooled compressible region, some manufacturers of pressure equipment recommend calculating the maximum allowable water mass using a safety factor and the ratio of ρ_L or its inverse v_L at the desired T to that at room temperature [20]. It is also important to note that the actual HTC pressure will be higher than that from the pure water because of gas production (predominantly CO_2) from HTC reactions.

Table 1. Example calculations for the effect of increasing the hydrothermal carbonization (HTC) temperature on reactor pressure for D = 865 kg/m^3 (values for saturated water properties taken from Lemmon et al. (2018).

Saturated Water (i.e., $VF_w < 1$)				
		200 °C	230	250
Specific volume of liquid water (v_l)	(m^3/kg)	0.00116	0.00121	0.00125
Specific volume of vapor water at (v_v)	(m^3/kg)	0.12721	0.07151	0.05008
Saturation pressure (P_{sat})	(MPa)	1.55	2.80	3.98
Subcooled Water (i.e., $VF_w > 1$)				
Liquid compressibility factor	(-)	0.010606	0.24601	0.39023
Reactor pressure (P) for D = 865 m^3/kg	(MPa)	2.00	49.44	81.55

2.2. HTC Reactor System

Three laboratory-scale HTC reactor systems were used to measure pressure change with temperature increase and validate the predicted values with experimental set-ups. Two sealed high pressure and temperature reactors made of Alloy C276 with valves and fittings made of T316 Stainless Steel (500-mL, Model 4575A and 1-L, Model 4680 HT, Parr Instrument Co., Moline, IL, USA) were used with various initial fillings with distilled water. A 1500-watts heater surrounding the outside reactor wall along with a programmable temperature controller was used to heat the reactants at a designed temperature. This reactor system was modified to improve control and data logging capability. In addition, a 18.75-L reactor system (Model 4555, T 316 Stainless Steel, Parr Instrument Co., Moline, IL, USA) with a similar heating system (6000 watts) and temperature controller (Model 4848BM) using SpecView data acquisition software was used to study the effect of initially pressurizing the system with nitrogen.

3. Results and Discussion

Understanding and replicating process conditions to produce a desired hydrochar quality require that we can estimate how much liquid water is in contact with the feedstock. Maintaining safe operating conditions requires that we can predict pressure increases during the reaction. In pressurized hydrothermal batch and semi-batch conversion systems, process conditions in the reaction system can be difficult to measure as well as to predict. The volume of liquid water and the distribution between the liquid and vapor phase change with temperature. Reactor pressure can increase with temperature due to (1) rising water vapor pressure, (2) the expansion of the liquid water, and (3) the production of process gas. In the following sections, the focus is on the effects caused by changes in the physical state of water. First, the relationships between temperature, pressure, the volume fraction of liquid water VF_w and the distribution of water between the liquid and vapor phase are shown for a reactor system filled only with water. Then, the evaluation is expanded to water and feedstock. Finally, the effect of these process conditions for VTC and HTC systems reported in the literature are discussed.

3.1. HTC Reactor Filled with Water Only

3.1.1. Estimating VF_w at Various Temperatures and VF_o

In HTC and VTC experiments, a wide range of initial water amounts can be used. For HTC experiments, high values of VF_o are commonly chosen. It is important, however, to choose process conditions so that the liquid water does not fill the reactor volume at the holding temperature (i.e., $VF_w = 1$) to avoid entering the subcooled liquid compression region. The higher the initial VF_o, the lower the reactor temperature at which VF_w becomes 1, because smaller headspace volumes cannot accommodate much expansion of liquid water as its density decreases with temperature. This behavior

is shown in Figure 2 for a reactor filled with water only. Values for VF_w were estimated at various temperatures and VF_o using Equation (4). For a reactor initially filled with water at 90% (i.e., $VF_o = 0.9$), the liquid volume expands to the reactor volume (i.e., $VF_w = 1$) when the reactor temperature reaches 165 °C. Fortunately, this critical temperature, at which $VF_w = 1$, increases rapidly as VF_o is decreased, e.g., 305 °C for $VF_o = 0.7$ and 365 for $VF_o = 0.5$, so that process conditions can be chosen to remain well below the critical temperature. When the reactor is initially filled with water to less than half its volume (i.e., $VF_o < 0.5$), the liquid does not fill the reactor even when the temperature approaches the critical point of water around 374 °C. Interestingly, for experiments with low values of VF_o common to VTC operating conditions, VF_w can actually decrease with temperature. When the reactor is initially filled with a very low volume of water, such as $VF_o = 0.1$, the liquid volume decreases to zero at $T = 340$ °C. This happens when there is so much headspace that the liquid water completely vaporizes, i.e., the molecular collision frequency of H_2O molecules in the headspace is so small that condensation does not happen in this high headspace situation.
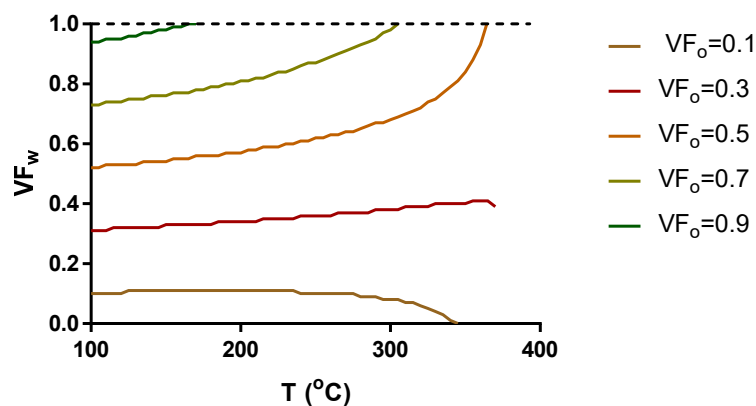

Figure 2. Change in volume fraction of reactor filled with liquid water VF_w (V_w/V_R) as a function of temperature for various initial liquid water volume fractions (VF_o).

3.1.2. Estimating Pressure and VF_w under Process Conditions

For a batch reactor system starting with only water at atmospheric pressure, the reactor pressure at the holding temperature can be easily estimated using the simple saturation water vapor pressure at T as long as $0 < VF_w < 1$. However, when $VF_w = 1$ or higher, if the temperature is further increased, the reactor pressure will now follow the subcooled water pressure, which rises rapidly. The pressure increase must then be estimated using Equation (5) with the liquid compressibility factor Z and the overall reactor water density D. This approach can then be used to predict the increase in reactor pressure as a function of the reactor temperature at various VF_o. The results are illustrated in Figure 3. When $VF_o = 0.3$, the liquid volume does not reach the reactor volume (i.e., $VF_w < 1$) even at the highest temperature simulated at 370 °C. Therefore, the reactor pressure follows the saturation water vapor pressure shown as the lower curve in Figure 3. For a reactor system with a high initial volume of water, e.g., $VF_o = 0.8$, the reactor pressure also follows the saturation pressure line below 250 °C, similar to the behavior at $VF_o = 0.3$. However, at $T = 250$ °C, VF_w becomes unity and the water enters the subcooled compression region. In this region, a small increase in temperature of only 5° can cause a rapid increase in pressure from 4.9 to 11.7 MPa (Figure 3).

The application of this approach to predict VF_w and pressure for experimental runs at various temperatures was evaluated by comparing the predicted pressures with the observed pressures in HTC reactors initially filled with three different amounts of water. As most researchers have discovered, determining the actual volume of an HTC reactor with cavity volume in the reactor head due to connections to the pressure gauge and sampling ports is difficult. Based on reactor volume estimations from simple geometric dimensions, the added water resulted in $VF_o = 0.3$, 0.63, and 0.67. For $VF_o = 0.3$, the observed pressures as the reactor was heated followed the saturation water vapor

line at temperatures up to 349 °C (Figure 3). However, for VF_o = 0.67 at temperatures higher than 349 °C, the pressure increased much more rapidly than the saturation vapor pressure, indicating that the water entered the subcooled compression region. According to the predicted pressure line for the estimated VF_o, it should have entered the subcooled region at a lower temperature of 320 °C. Instead, the observed pressure followed the predicted pressure line of VF_o = 0.6 (Figure 3). We suspect that this discrepancy can be attributed to the fact that the actual reactor volume was larger than the estimated volume, (e.g., 1.1 L instead of 1 L for 0.67 L water initially filled). These results show that the approach is adequate to estimate VF_w at various reactor temperatures in practical applications, however, if the actual reactor volume is not known accurately, there will be some deviation from the predicted values.
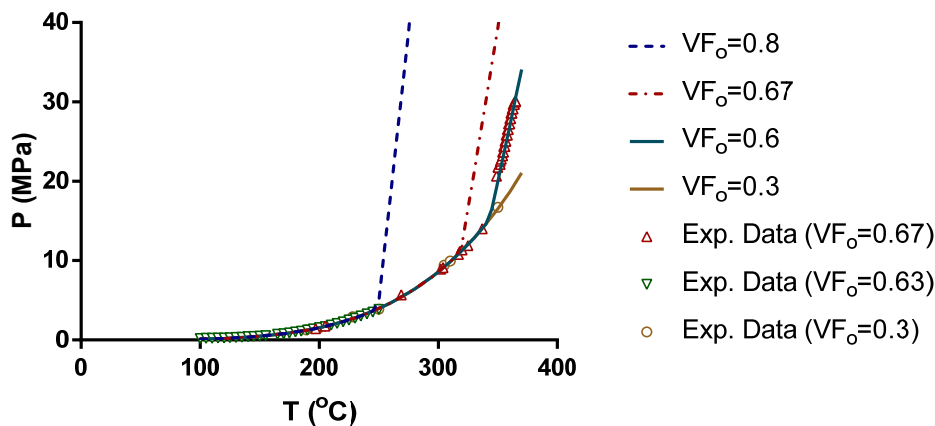

Figure 3. Comparison of measured and estimated reactor pressure at different initial liquid water volume fractions (VF_o).

Another important question to consider in deciding upon operating conditions and evaluating experimental results is: How does a higher initial pressure affect the pressure development and phase distribution of water in the reactor? For example, some experimenters pressurize the system initially using an inert gas such as N_2 or Ar. The answer in short is that the addition of pressure to the reactor headspace does not change the behavior of water. If enough water and time are available, water will vaporize to the gas phase to reach the saturation water vapor pressure at which liquid water and vapor water are in equilibrium. This pressure is a function of temperature only and independent of the presence of other gases. The added inert gas does not change the relationships for VF_w and the distribution of water between the liquid and vapor phases. However, the total reactor pressure will be higher in the reactor initially filled with N_2 or Ar than that without the initial inert gases. The total pressure *P(total)* can be estimated by summing the partial pressures of all individual non-reacting gases as stated in Dalton's law. The increase in the partial pressure for each component with temperature can be calculated independently and added together. This can be seen in Figure 4 for two experimental runs in an 18.75-L Parr reactor in which water was heated to 220 °C (VF_o = 0.63): one starting at atmospheric pressure and the second one with N_2 addition to achieve an initial pressure of 1.4 MPa. The measured values from the nonpressurized run (P_o = 0.1 MPa) are compared to the saturation water vapor pressure *P(sat)* from [2] in the lower curve. For the run at P_o = 1.4 MPa, the partial pressure increase for N_2 $P(N_2)$ was estimated using the ideal gas law, combined with Equation (4) to calculate the changes in headspace volume ($1-VF_w$) as temperature increases.

Comparison of the measured and theoretical values shows clearly that the contribution of the saturated water vapor to the total pressure is not affected by the initial addition of N_2 gas. The small deviation between the calculated pressure and the measured can be due to inaccuracies in the pressure measurement or in estimating the reactor volume, and the assumption that N_2 behaves as an ideal gas with no solubility in the liquid. Nevertheless, the difference does not mask that the fact that the addition of pressure to the reactor headspace does not change the behavior of water.
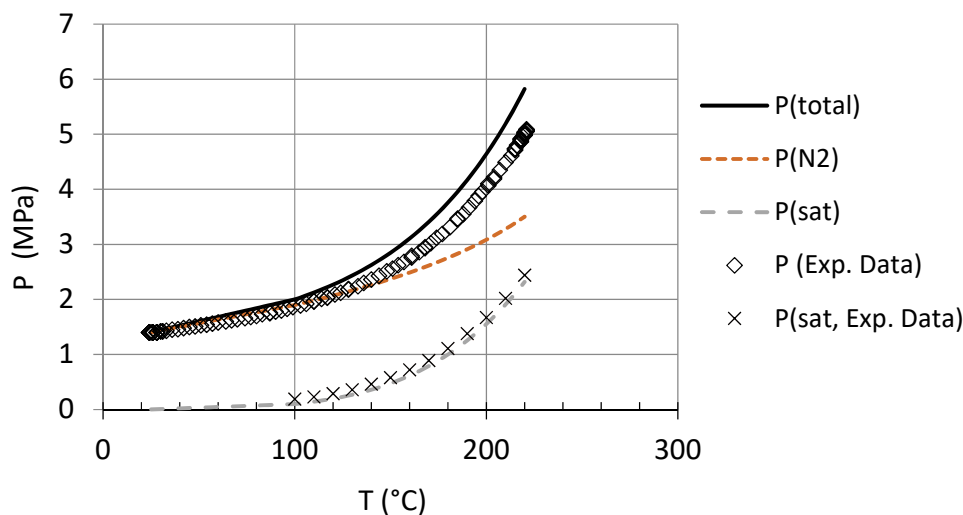
Figure 4. Comparison of the theoretical total pressure *P(total)* calculated from the partial pressures for N$_2$ *P(N$_2$)* and saturated water vapor *P(sat)* to the measured values for pressure *P* and *P(sat)* in the reactor for *VF$_o$* = 0.63.

3.2. HTC Reactor Filled with Water and Feedstock

3.2.1. Estimating the Distribution of Water between Phases as a Function of Temperature and Its Effect on Solid Content

In their comparison of hydrochars from VTC and from HTC systems, Cao et al. (2013) postulated that the amount of liquid water in contact with the feedstock in the reaction system may determine the degree of carbonization and influence which reactions take place and their sequence [5]. However, they did not quantify how much liquid water was in contact with the feedstock in their reaction systems. This is a common problem in most of the literature on HTC/VTC systems. Often the label used for the system is defined by the initial conditions. For instance, when the feedstock is initially completely submerged in bulk liquid water, it is commonly called an HTC system. Whereas, when dry or wet feedstock is placed separately from the bulk liquid water, it is called a VTC system. However, the volume of liquid water and the distribution of water between the liquid and vapor phase change with temperature, which can change the amount of water contacting the feedstock. In addition, the feedstock characteristics such as moisture content, particle size, bulk density, as well as structural changes during the reaction can affect how water interacts with the feedstock. In VTC, carbonization reactions can take place between a wet feedstock and water within its cells or present as a film on its surface [10,11]. Ref. [11] Even with completely dried feedstock, the feedstock can be wetted during the process by absorbing water vapor or water vapor condensing on its surface.

The parameters often used to describe the relationship between water and feedstock in a reaction system do not differentiate between the bulk liquid water added to the process and the liquid water in contact with the feedstock. The nominal solid content at the start of the run is usually reported in published studies as:

$$\%S_o = \left(\frac{M_{biomass}}{M_{H2O} + M_{biomass}} \right)_{T=T_o} \times 100 \tag{6}$$

where

$\%S_o$ = nominal solid content;

$M_{biomass}$ = initial feedstock dry mass;

M_{H2O} = total mass of water in the reactor.

A similar parameter *R* which describes the initial ratio of feedstock dry mass to total mass of water is also often used. These parameters only describe the initial conditions based on the initial filling masses of water and feedstock, but do not provide critical information on the extent to which

feedstock is exposed to liquid water in the HTC or VTC systems to promote important hydrothermal carbonization reactions. In order to provide useful information on the degree of physical contact between the feedstock and liquid water throughout the process, we propose reporting the following solid content parameter:

$$\%S(T) = \left(\frac{M_{biomass}}{m_{H2O} + M_{biomass}}\right)_{T=T} \times 100 \tag{7}$$

where

$\%S(T)$ = actual solid content based on liquid water in contact with feedstock;

m_{H2O} = mass of liquid water in contact with feedstock;

T = reactor temperature.

With these new definitions, one can systematically distinguish various HTC/VTC process conditions in terms of fraction of liquid water physically in contact with feedstock. For HTC systems, where the feedstock is assumed to be completely submerged in the bulk liquid water over the whole reaction time, $m_{H2O} = x_L \cdot M_{H2O}$. Using Equations (3) and (4), these assumptions can be checked for the reaction temperature and the solid content values adjusted with Equation (7). For example, the change in the distribution of water between the two phases can be seen in Figure 5a. For temperatures below 250 °C and VF_o larger than 0.3, less than 4% of the water will be vaporized. The expansion of VF_w, as seen in Figure 2, should offset the small loss of liquid water to the vapor phase and submerged feedstocks should remain submerged at these conditions. Therefore, the actual solid content will be approximately the same as the nominal solid content at the initial reactor temperature T_o (i.e., $\%S(T) = \%S_o$). Only for systems with VF_o closer to 0.1, more common to VTC systems, will approximately 20% of the water be present as vapor at 250 °C.
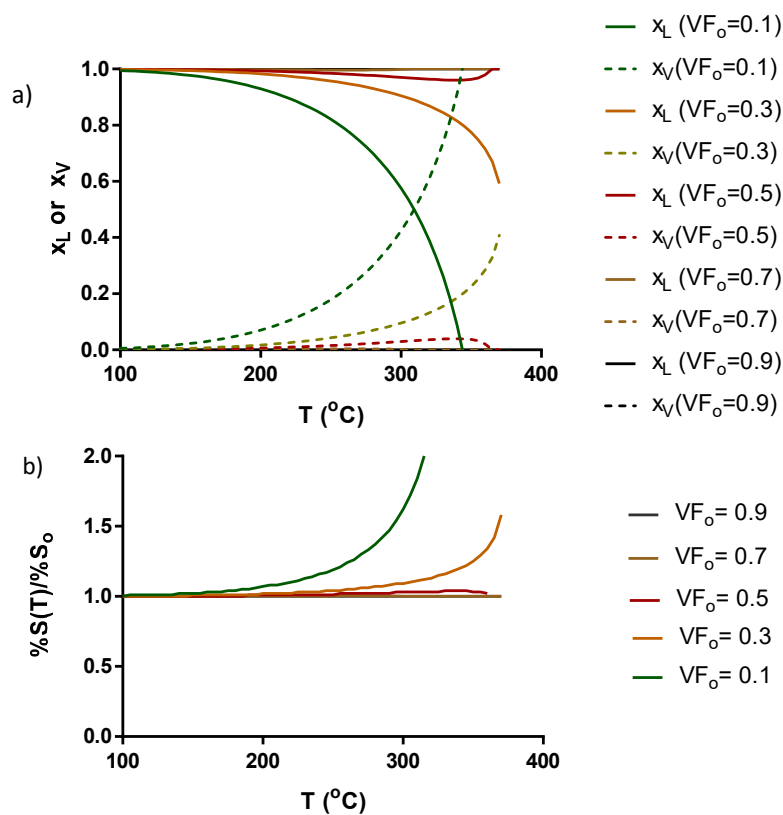

Figure 5. Changes in process parameters at various initial VF_o as the operating temperature increases for (**a**) mass fractions of water in liquid x_L and vapor x_V, (**b**) the ratio of actual to nominal solid content in the reactor system, $\%S(T)$ at T to $\%S_o$ at the initial temperature.

In VTC systems, wetted or completely dried feedstock can be suspended without any physical contact with bulk liquid water. The bulk liquid water can be placed either at the bottom of the reactor or in a separate interconnected chamber, or steam can be injected to heat the reactor. The value reported for $\%S_o$ for such systems often includes the bulk water. However, this can be misleading, especially for dried feedstock, where the actual initial solid content $\%S(T_o) = 1$ because $m_{2O} = 0$. Although $\%S(T_o) = 1$ initially, $\%S(T)$ will become less than one over time because water vapor will be volatilized from the physically separated bulk liquid as the VTC reactor temperature increases and will condense on the surface of the dry feedstock. The extent to which the vaporized water condenses onto the feedstock depends on the kinetics of condensation and vaporization at the reaction temperature, but $\%S(T)$ will rarely reach $\%S_o$. The condensed water will promote typical hydrolysis and other important carbonization reactions as in HTC systems. For VTC systems with initially wetted feedstock, bulk liquid water may or may not be added to the reactor. If no bulk liquid water is added similar to that of Funke et al. [11], $\%S(T_o) = \%S_o$, where the moisture content (*MC*) determines the value of the initial solid content. As the temperature increases, liquid water is lost to vaporization, reducing the water content of the feedstock. $\%S(T)$ can then be calculated with Equation (7) and:

$$m_{H2O} = x_L \times M_{H2O} = x_L \times \frac{M_{biomass} \times MC}{1 - MC} \tag{8}$$

Using these equations for the new solid content parameters, the ratios of actual to nominal solid content are plotted against the reactor temperatures in Figure 5b for various initial volume fractions of liquid water. For HTC systems with VF_o larger than 0.3 and temperatures below 250 °C, there is little difference between the two values. At 250 °C, only a 4% increase is seen in $\%S(T)$, and after the reactor is half-filled (i.e., $VF_o > 0.5$), no differences are noticeable. In contrast, for systems with low values of VF_o (e.g., $VF_o = 0.1$), $\%S(T)$ becomes 20% higher than $\%S_o$. Less liquid water is in contact with the solids to participate in reactions. For VTC systems with wet feedstocks where the liquid water is associated in or on the feedstock, the transfer of water to the vapor would change the $\%S(T)$ in the reactor significantly. For wetted feedstock suspended over bulk liquid water, the situation is more complicated, since water can vaporize from the wet feedstock or bulk liquid water, mass transfer within and in-between feedstock, and the kinetics of condensation and vaporization all play roles in the location of the liquid water. This is beyond the scope of this paper. Moreover, the implications of the reduction in the mass of bulk liquid water on the potential of reducing physical contact between feedstock with a bulk volume larger than that of liquid water and subsequent carbonization reactions need to be further studied.

3.2.2. Estimating VF_w and Pressure under Process Conditions with Feedstock

Up until now. we have analyzed the changes in volume fractions due to changes in the physical properties of water. The addition of feedstock to the reactor can reduce the headspace volume available to accommodate the expansion of liquid water. To adjust the volume fractions for the presence of feedstock, the reactor volume must be reduced by the volume occupied by the feedstock. To strictly determine this volume, we need to know the true density of the material, i.e., the ratio between the feedstock mass and its volume excluding the cavities, pores and gaps in the material where water and air could be trapped. In addition, the loss of solid mass and structure during HTC reactions would have to be taken into consideration. For practical purposes, simple estimates of the initial volume of feedstock can be made with liquid displacement methods and used to adjust the calculation of VF_w.

HTC reactions with the feedstock can also change the gas composition and pressure of the headspace. The composition and amount of the produced gases is closely tied to the process conditions and feedstock material. In general, most HTC reactions with biomass produce predominantly CO_2 (~>80%) with minor percentages of N_2, H_2S, O_2, CH_4, H_2, etc., in the gas besides water vapor. Explosive gas mixtures are not expected in HTC, unlike hydrothermal gasification where reactor temperatures are near or above the critical temperature of water (i.e., ~374 °C) and produce approximately 1:1 of CH_4

and CO_2. However, an in-depth analysis about gas production and compositions is beyond the scope of this paper. The impact of the product gas on the total reactor pressure and its partition between water and gas phases need to be further investigated as gas solubility changes with temperature and pressure. The results of this study provide a theoretical framework for further experimental and modeling research on this aspect of HTC.

3.3. Comparison of Process Conditions for Hydrothermal Treatment (HTC and VTC) Reported in the Literature

The results from published HTC/VTC studies that have been made at various scales, ranging from 1 L to 10 m^3, and with different modes of operation, e.g., batch and semi-batch with respect to the steam, are analyzed in this section. As summarized in the introduction, few studies comparing HTC and VTC systems have been published and some results are contradictory. The goal here is to identify the effect of process conditions on the distribution of the water between the phases to understand what is behind the labels—HTC and VTC—and develop criteria on how to label systems, either HTC or VTC. This is necessary especially for cases in which we want to replicate process conditions used to produce a desired hydrochar quality in other reactor types and/or scales. The results are structured into seven cases for the discussion here and an overview of the process conditions and feedstocks is given in Table 2.

Table 2. Overview of the process conditions and feedstock for the seven cases with VTC/HTC processes.

Case	Reactor					Feedstock			Water in System		Literature
	Type	T (°C)	V_R (L)	Heating	Mixed	Type	MC (%)	$M_{biomass}$ (gDM)	M_{H2O} (g)	v_R (m^3/kg)	
1	Batch HTC	200	1	heating band	No	bark	7	23.5	101.6	0.010	Cao et al. [5]
						sugar beet	7	37.6	162.9	0.006	
2	Semi-batch VTC	200	70	steam, condensate removal	No	bark	40–70	n.r.	n.r.	0.013 *	
						sugar beet	40–70	n.r.	n.r.	0.012 *	
3	Semi-batch VTC	200	10,000	steam, no condensate removal	Yes	MSW	53	1771.9	start 1998.1	start 0.005	Safril et al. [9]
									end 3398.1	end 0.0029	
4	Batch HTC	230	18.75	heating band	No	wheat straw	0	450	8550	0.00219	Funke et al. [11]
						digestate	0	630	11,970	0.00157	
5	Batch VTC	230	18.75	heating band	No	wheat straw	25	450	1350	0.01390	
						digestate	25	630	1890	0.00995	
6	Batch HTC	220	4.6	heating band	No	bagasse	67.2	16.6–28.8	1495.5	0.003	Shafie et al. [10]
						lime peel	78	14.4–44.0	1495.5	0.003	
7	Semi-batch VTC	220	4.6	heating band, condensate separated	No	bagasse	67.2	n.r.	n.r.	0.041–0.053 [@]	
						lime peel	78	n.r.	n.r.	0.022–0.044 [@]	

n.r.—not reported. *MC* – moisture content. * Assumed *50% reactor volume filled with bark or sugar beet feedstock (MC = 55%) suspended in baskets with bulk density of 0.267 kg/L for bark [21] and 0.298 kg/L for sugar beet pulp [22].* [@] Assumed the same amount of feedstock as in Case 6 with biomass bulk density of 0.616 kg/L for bagasse [23] and 0.490 kg/L for lime peel [24].

In Cases 1 and 2, a comparison of batch HTC (Case 1) with semi-batch VTC (Case 2) using the same feedstocks was made in different reactor systems [5]. For Case 1, the feedstock was dried, ground, and water added to the 1 L reactor, submerging the feedstock. In Case 2, the wet feedstock was suspended in baskets and steam (1.6 MPa) was injected to heat the 70 L reactor. As water condensed over the heating up and holding time, it was removed except for that which remained on the feedstock. Therefore, there was no increase in the mass of condensed water in the reactor over time (Revatec GmbH, DE 10 2009 010 233.7). The feedstock was reported to have a moisture content between 40 and 70%. For the calculations here, the mass of water in the system was estimated from the overall specific volume of saturated water vapor at 200 °C in the 70 L reactor and an average moisture content of the feedstock (55%) during the HTC reaction. As feedstock loading information is not available, we assumed 50% of the reactor volume was filled with bark or sugar beet pulp suspended in baskets

inside the reactor. The mass of water was estimated using bulk densities of bark and sugar beet pulp reported in the literature [21,22].

In Case 3, a commercial-scale hybrid system with municipal solid waste (MSW) in a 10 m^3 reactor system was used [9]. The semi-batch system was fed saturated steam (2.5 MPa) to heat the feedstock and held at 180–230 °C for 30 min. The system started similar to a VTC system with only wet feedstock, but as the condensed steam was mixed with the feedstock over time, the system became more similar to HTC. A mid-range temperature of 200 °C was assumed for further analyses here. In Cases 4 and 5, Funke et al. compared VTC and HTC for two feedstocks in the same batch reactor system [11]. For VTC, the dried feedstock was first soaked in water and then suspended in a basket without any additional liquid water added to the reactor. For HTC, the dried feedstock was submerged in water. In Cases 6 and 7, Shafie et al. used bagasse with *MC* of 67.16% (cut into less than 10 mm) and lime peel with *MC* of 78.04% (size as received) as feedstock [10]. For HTC, the feedstock was fully submerged inside the water in a reactor. For VTC, saturated steam was supplied to the reactor with the feedstock suspended in order to avoid contact with condensed liquid water accumulated at the bottom of the reactor. As feedstock loading information was not reported for the VTC experiments, we assumed the mass of feedstock was the same as that used in HTC experiments, along with bulk densities from the literature (bagasse [23]; lime peel (value for lemon peel was used [24]). The process conditions and feedstock for each case are summarized in Table 2, along with the respective v_R, overall specific volume of reactor liquid water and steam mixture.

3.3.1. Change in Process Conditions in Batch HTC (Cases 1, 4, 6) or VTC Processes (Case 5)

In batch reactors, the solids and liquids are introduced at the beginning of the run and the reactor is sealed before heating starts. The initial VF_o and $\%S_o$ can be easily calculated and are usually reported (Table 3). Feedstock initially submerged in water can unequivocally be called HTC when VF_w at the holding temperature remains as large or larger than VF_o. This is true for all batch HTC cases (1, 4, 6) analyzed here. Each case includes results for two feedstocks under slightly differing conditions. In Case 4, with a relatively large amount of initial water (VF_o = 0.46 and 0.64, for wheat straw and digestate, respectively), the expansion of water at 230 °C causes VF_w to increase by approximately 20%. As only 0.5 to 1.4% (m/m) of the initial liquid water is transferred to the vapor phase, there is little to no change in $\%S(T)$. Similarly, very little increase in solid content is observed in Case 6. In contrast, Case 1 at 200 °C has a low degree of initial water filling for both feedstocks (i.e., VF_o = 0.1 and 0.16), and VF_w is very similar to VF_o. Between 4 and 7% of the water is transferred to the vapor, causing a corresponding increase in the value of $\%S(T)$. The values for $\%S(T)$ ranged from 1.0 to 19.9% for all batch HTC cases, ensuring adequate contact with liquid water to promote HTC reactions. Despite the loss of liquid water due to vaporization, the filling volume (VF_w) slightly increases because the volume of water expands with the reactor temperature, guaranteeing that the feedstock is completely submerged in the liquid water throughout the reaction period. Therefore, hydrothermal reactions will take place between the feedstock and liquid water and the process can be called batch HTC in Cases 1, 4, and 6.

If the solids are suspended in the reactor in baskets or on trays so that they are not submerged in water, the process is commonly called VTC (Cases 5). If the feedstock has a high moisture content such as the dried feedstock soaked in water (Case 5, *MC* = 75% or $\%S_o = \%S(T_o) = 25\%$), or it is made up of intact microorganisms or fresh plant material, the actual $\%S(T)$ slightly increases compared to $\%S_o$ (27.6 or 28.9 vs. 25%) due to the small loss of liquid water in the feedstock to vapor (Table 3).

Table 3. Overview of process conditions and water distribution for the seven cases of VTC/HTC.

Case	Reactor	Feedstock	v_R	Mass Fraction in Vapor x_v	VF_o	VF_w	$\%S_o$	$\%S(T)$
	Type	Type	(m^3/kg)	(-)	(-)	(-)	(%)	(%)
1	Batch HTC	bark	0.010	0.069	0.1	0.11	18.8%	19.9%
		sugar beet	0.006	0.04	0.16	0.18	18.8%	19.4%
2	Semi-batch VTC	bark	0.013 *	0.051 *	n.r.	-	45%[#]	45% [#]
		sugar beet	0.012 *	0.046 *	n.r.	-	45%[#]	45% [#]
3	Semi-batch VTC	MSW	start 0.005	start 0.03	0.2		47.0%	
			end 0.0029	end 0.0142		0.34		34.6%
4	Batch HTC	wheat straw	0.00219	0.014	0.46	0.54	5.0%	5.1%
		digestate	0.00157	0.0051	0.64	0.77	5.0%	5.0%
5	Batch VTC	wheat straw	0.01390	0.1804	0.07	0.07	25.0%	28.9%
		digestate	0.00995	0.1239	0.1	0.11	25.0%	27.6%
6	Batch HTC	bagasse	0.003	0.03	0.33	0.378	1.1–1.9%	1.1–2.0%
		lime peel	0.003	0.03	0.33	0.378	1.0–2.9%	1.0–3.0%
7	Semi-batch VTC	bagasse	0.041–0.053 [@]	0.473–0.609 [@]	n.r.	-	32.8%	32.8%
		lime peel	0.022–0.044 [@]	0.251–0.510 [@]	n.r.	-	22.0%	22.0%

n.r.—not reported. * Assumed 50% of reactor volume filled with bark or sugar beet suspended in baskets. [#] Averaged value for feedstock. [@] Assumed the same amount of feedstock as in Case 6.

3.3.2. Change in Process Conditions for Semi-Batch VTC Process with Steam Injection (Cases 2 and 7 with Condensate Removal or Separation, and Case 3 without Condensate Removal)

For reactors in Cases 2 and 3 with a semi-batch mode of operation where saturated steam is introduced over time to first heat the reactor and then to maintain the desired operating temperature, the calculations for how much mass of the water is present as liquid or vapor are not as straightforward. The steam condenses as it heats the feedstock to the targeted operating temperature, and more will condense over the targeted holding time. As steam is introduced, the reactor pressure will remain constant at the saturation pressure if there are no reaction products entering the vapor phase. However, gases are normally produced by the hydrothermal reactions and the pressure rises as the gases, mainly CO_2, enter the headspace.

For systems with condensate removal, as in Case 2, or condensate separation, as in Case 7, the mass of bulk liquid water in contact with feedstock comes from moisture already present within the feedstock and water condensation on the surface of feedstock. Wet feedstocks will retain most of their moisture. For dried feedstock, the majority of the water in the system will be in the vapor, with some steam condensing on the feedstock surface, especially in the heating phase. Assuming that the amount of steam condensed on the feedstock surface is negligible, the overall specific volume v_R is mostly that of the saturated water vapor and the moisture content of the feedstock. In such systems, the process can be labeled VTC without much ambiguity. The amount of liquid water that can react with the feedstock for VTC systems mainly depends on the moisture content of the original feedstock and the condensed water on the feedstock surface. It is very difficult to quantify this amount of water. For these two cases, $\%S(T)$ was assumed to remain the same as the initial value. The condensed water is sometimes flashed off at the end of the run (e.g., for energy recovery (Revatech, 2012)), so that the solids come out about as wet as they went in. This is helpful in reducing dewatering requirements, but this hinders easily assessing how much water was in contact with the feedstock.

In systems without condensate removal, as in Case 3, the continuous injection of steam will build up the total mass of water in the system, with the majority present in the form of liquid water. The VTC process then approaches the HTC process. In this hybrid VTC–HTC commercial-scale unit, the reaction system is well-mixed and liquid water is mixed into the feedstock, gradually lowering the value of $\%S(T)$ in the reactor from the initial $\%S_o$ value 47% to 34.6%. The volume fraction of vapor water (x_V) changes somewhat. Starting with 3% of the water present as vapor, it reduces to 1.4% at the end of the run (Table 3). In general, it is important to measure the mass of steam introduced in systems without

condensate removal, so that the mass of accumulated condensed water can be monitored as a safety precaution. Steam injection must stop before VF_w approaches 1 to avoid rupture of the reactor.

It is interesting to note that the solid content *%S(T)* of feedstock for all seven cases was less than 45% at the reaction temperature. The solid content for HTC systems ranged from 1.0 to 19.9%, while that for VTC systems from 27.6 to 45%. It means that 55% or more of the total water mass was present as liquid water and had direct physical contact with feedstock promoting carbonization reactions. According to Cao et al., the lower the *%S(T)*, the more the product was carbonized. The highest solids content for VTC was 45% in Case 2 because of the water already present within the raw feedstock even though additional water was not supplied. This leads to questions on what will happen if we conduct VTC with completely dried feedstock, such as: Is it possible to carbonize the dried feedstock with steam alone? For such reaction systems, the initial value of *%S(T$_o$)* equals one. The value of *%S(T)* will become less than one as some of the steam condenses on the surface of feedstock promoting the HTC reactions. In such a system, the extent of carbonization will be determined by the extent of the wetting of the feedstock by steam. More detailed study is needed to understand the relationship between the degree of wetting by steam and carbonization.

3.4. Comparison of the Processes Using the T–v Diagram

To graphically illustrate the process conditions for each case at its reaction temperature, the values for the seven cases are plotted on a *T-v* phase diagram (Figure 6). Their locations in relation to the saturation curve show whether steam or liquid water predominates at the specific process conditions. Due to the log scale for the x-axis, the ratio between the two phases cannot easily be determined visually from the figure. Nevertheless, this visualization may help us to understand why some results from these studies comparing HTC and VTC systems are contradictory. The operating conditions in the HTC vs. VTC comparative studies are very different. The thermodynamic conditions in Cases 4 and 6 result in water being present mainly as a liquid for the HTC reactions as expected (i.e., toward the left side of the dome), while Case 5 is mid-range and Case 7 is located nearer the vapor saturation curve with a predominant steam phase. Process conditions for Case 1 (HTC) are to the left of Case 2 (VTC) on the 200 °C and 1.5 MPa isobaric line, suggesting more HTC reactions in Case 1, but the locations are closer together than the other pairs. Thus, this diagram visualizes the differences in the reaction phases, and allows us to subsequently interpret whether the system can be characterized more as HTC or VTC. When the conditions result in the same overall specific volume but with different process temperatures, the amount of water present as steam will change. This is true for Case 1-bark and Case 5-digestate (Table 3 and Figure 6). Both have a similar v_R, but Case 5-digestate at 230 °C has almost double the amount of water present as steam ($x_v = 0.1239$) than that for Case 1-bark at 200 °C ($x_v = 0.069$).
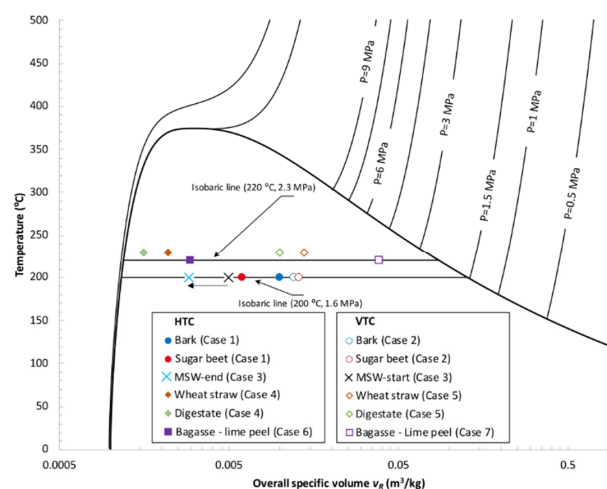

Figure 6. Comparison of the process conditions for the seven cases in the *T–v* diagram for water.

Furthermore, the diagram helps visualize the safety aspects. It is easy to see that the target conditions in Cases 1, 2, 5, and 7 are well away from entering the subcooled liquid compression region, where pressure increases rapidly with an increase in reactor temperature. For the semi-batch system in Case 3, the overall specific volume v_R decreases from 0.005 to 0.0029 m^3/kg due to the increase in the total mass of water as steam is injected into the reactor, and we move from the right to the left on the isobaric line at 1.6 MPa (Figure 6). For such semi-batch systems, it is important to make sure the start and end points remain far enough away from the subcooled compression region. Temperature increases above the initial target conditions due to use of superheated steam or exothermic reactions could move the system diagonally upwards towards the subcooled compression region and high pressure as steam is added. In the subcooled compression region, if a safety rupture disk valve is not present to release at a preset pressure, the reactor pressure can exceed the tensile strength of reactor material, and the reactor can explode.

4. Conclusions

There are many types of hydrothermal reactor systems being used with many process variations in the literature. The analysis presented in this paper illustrates that a large range of conditions need to be considered before labeling a reactor system VTC and HTC. The analysis of the process conditions of seven different HTC/VTC cases reported in the literature through the use of the models developed in this paper and a *T-v* phase diagram showed that the distinction between HTC and VTC is often ambiguous. The models developed in this study for predicting pressure, the volume fraction of liquid water and the distribution of water between phases as a function of reactor temperature can be used to systematically analyze various HTC/VTC process conditions. Furthermore, this study also demonstrates the importance of predicting the condition at which the reactor system enters the subcooled compression liquid region to avoid the danger of explosion. Comparison of the reactor pressures predicted by the models to the actual pressure for reactors filled with varying amounts of water with and without initial pressurization showed reasonable agreement. However, higher pressures can be expected with the addition of feedstock due to the production of CO_2 and other gases by the hydrothermal reactions and the decrease in headspace volume occupied by the feedstock. In order to describe the amount of liquid water in physical contact with feedstock, we defined a new solid content parameter *%S(T)* which changes with reaction temperature due to changes in the water distribution between phases. This parameter is more useful in describing the solid content than the nominal parameter *%S$_o$* typically reported in the literature. While the models developed here can help determine whether steam or liquid water predominates at the specific process conditions, more research and modeling on hydrothermal systems with feedstock present are required to understand the effect of the water phase on the hydrothermal reactions. The tools presented here can help in designing experiments to compare systems and in understanding results in future HTC research.

Glossary

Symbol	Description	Unit
D	overall reactor water density, M_{H2O}/V_R	kg/m^3
$M_{biomass}$	mass of feedstock in the reactor as dry matter (DM)	
M_{H2O}	total mass of water as liquid and vapor water in the reactor	kg
MC	moisture content	%
MW_{H2O}	molecular weight of water	kg/kmol
P	reactor pressure	MPa
P_o	initial reactor pressure	MPa
P_{sat}	saturated vapor pressure	-
R	universal gas constant (8.31451×10^{-3} m^3-MPa/kmol-K)	-
$\%S$	% solid in reactor—ratio of mass of feedstock in DM to (total mass of water + mass of feedstock in DM in reactor), $M_{biomass}/(M_{H2O} + M_{biomass})$	-
T	reactor temperature	°C
VF_o	volume fraction of liquid water in the reactor at initial temperature T_o	-
VF_w	volume fraction of liquid water in the reactor at temperature T	-
V_R	reactor volume	m^3
V_w	volume of liquid water in the reactor at temperature T	m^3
v_R	overall specific volume of reactor liquid water and steam mixture, V_R/M_{H2O}	m^3/kg
v_L	specific volume of saturated liquid water	m^3/kg
v_v	specific volume of saturated steam	m^3/kg
x_L	mass fraction of liquid water	-
x_v	mass fraction of vapor water or steam (or also called steam quality)	-
Z	compressibility factor for liquid or vapor	-

References

1. Libra, J.A.; Ro, K.S.; Kammann, C.; Funke, A.; Berge, N.D.; Neubauer, Y.; Titirici, M.M.; Fuhner, C.; Bens, O.; Kern, J.; et al. Hydrothermal carbonization of biomass residuals: A comparative review of the chemistry, processes and applications of wet and dry pyrolysis. *Biofuels* **2011**, *2*, 71–106. [CrossRef]

2. Cao, X.; Ro, K.S.; Chappell, M.; Li, Y.; Mao, J. Chemical structures of swine-manure chars produced under different carbonization conditions investigated by advanced solid-state 13C nuclear magnetic resonance (NMR) spectroscopy. *Energy Fuels* **2011**, *25*, 388–397. [CrossRef]

3. Ro, K.S.; Flora, J.R.V.; Bae, S.; Libra, J.A.; Berge, N.D.; Álvarez -Murillo, A. Properties of animal-manure-based hydrochars and predictions using published models. *ACS Sustain. Chem. Eng.* **2017**, *5*, 7317–7324. [CrossRef]

4. Roman, S.; Libra, J.A.; Berge, N.D.; Sabio, E.; Ro, K.S.; Li, L.; Ledesma, B.; Alvarez, A.; Bae, S. Hydrothermal carbonization: Modeling, final properties design and applications: A review. *Energies* **2018**, *11*, 216. [CrossRef]

5. Cao, X.; Ro, K.S.; Libra, J.A.; Kammann, C.; Lima, I.M.; Berge, N.D.; Li, L.; Li, Y.; Chen, N.; Yang, J.; et al. Effects of biomass types and carbonization conditions on the chemical characteristics of hydrochars. *J. Agric. Food Chem.* **2013**, *61*, 9401–9411. [CrossRef] [PubMed]

6. Ro, K.S.; Novak, J.M.; Johnson, M.G.; Szogi, A.A.; Libra, J.A.; Spokas, K.A.; Bae, S. Leachate water quality of soils amended with different swine manure-based amendements. *Chemosphere* **2016**, *142*, 92–99. [CrossRef] [PubMed]

7. Minaret, J.; Dutta, A. Comparison of liquid and vapor hydrothermal carbonization of corn husk for the use as a solid fuel. *Bioresour. Technol.* **2016**, *200*, 804–811. [CrossRef] [PubMed]

8. Álvarez-Murillo, A.; Roman, S.; Ledesma, B.; Sabio, E. Study of variables in energy densification of oliver stone by hydrothermal carbonization. *J. Anal. Appl. Pyrolysis* **2015**, *113*, 307–314. [CrossRef]

9. Safril, T.S.; Safril, B.I.; Yoshikawa, K. Commercial demonstration of solid fuel production from municipal solid waste employing the hydrothermal treatment. *Int. J. Environ. Sci.* **2017**, *2*, 316–323. [CrossRef]

10. Shafie, S.A.; Al-attab, K.A.; Zainal, Z.A. Effect of hydrothermal and vapothermal carbonization of wet biomass waste on bound moisture removal and combustion characteristics. *Appl. Therm. Eng.* **2018**, *139*, 187–195. [CrossRef]

11. Funke, A.; Reebs, F.; Kruse, A. Experimental comparison of hydrothermal and vapothermal carbonization. *Fuel Process. Technol.* **2013**, *115*, 261–269. [CrossRef]

12. Berge, N.D.; Ro, K.S.; Mao, J.D.; Flore, J.R.V.; Chappell, M.A.; Bae, S. Hydrothermal carbonization of municipal waste streams. *Environ. Sci. Technol.* **2011**, *45*, 5696–5703. [CrossRef] [PubMed]

13. Gomez, J.; Corsi, G.; Pino-Cortes, E.; Diaz-Robles, L.A.; Campos, V.; Cubillos, F.; Pelz, S.K.; Paczkowsk, S.; Carrasco, S.; Silva, J.; et al. Modeling and simulation of a continuous biomass hydrothermal carbonization process. *Chem. Eng. Commun.* **2020**, *207*, 751–768. [CrossRef]

14. Yeoh, K.-H; Shafie, S.A.; Al-attab, K.A.; Zainal, Z.A. Upgrading agricultural wastes using three different carbonization methods: Thermal, hydrothermal and vapothermal. *Bioresour. Technol.* **2018**, *265*, 365–371. [CrossRef] [PubMed]

15. Akiya, N.; Savage, P.E. Roles of water for chemical reactions in high-temperature water. *Chem. Rev.* **2002**, *102*, 2725–2750. [CrossRef] [PubMed]

16. Lemmon, E.W.; Bell, I.H.; Huber, M.L.; McLinden, M.O. *NIST Standard Seference Database 23: Reference Fluid Thermodynamic and Transport Properties-REFPROP, Version 10.0*; National Institute of Standards and Technology (NIST): Gaithersburg, MD, USA, 2018.

17. Lemmon, E.W.; McLinden, M.O.; Friend, D.G. Thermophysical properties of fluid systems. In *NIST Chemistry Webbook*; NIST Standard Reference Database No. 69; National Institute of Standards and Technology (NIST): Gaithersburg, MD, USA, 2017.

18. IAPWS Thermodynamic Property Formulations. Available online: http://www.iapws.org/newform.html (accessed on 1 October 2020).

19. Parr Stirred Reactors and Pressure Vessels. Chapter 2. Bulletin 4500, Volume 12. Available online: https://www.parrinst.com/de/files/downloads/2013/08/4500MB-v12.0_Ch2_Parr_Stirred-Reactors-Literature.pdf (accessed on 15 May 2020).

20. Parr Safety in the Operation of Laboratory Reactors and Pressure Vessels. No. 230M, 8; Moline, IL. 2009. Available online: https://www.ccmr.cornell.edu/wp-content/uploads/sites/2/2015/11/ParrReactorSafetyInfo-230m.pdf (accessed on 15 May 2020).

21. Corder, S.E. Properties and uses of bark as an energy source. In Proceedings of the XVI IUFRO World Congress, Oslo, Norway, 20 June–2 July 1976; Volume 31.

22. Karpaky, H.; Maalouf, C.; Bliard, C.; Gacoin, A.; Lachi, M.; Polidori, G. Mechanical and thermal characteriziation of a beet pulp-starch composite for building applications. *E3S Web Conf.* **2019**, *85*, 1–8. [CrossRef]

23. Oliveira, S.L.; Mendes, R.F.; Mendes, L.M.; Freire, T.P. Particleboard panels made from sugarcane bagasse: Characterization for use in the furniture industry. *Mater. Res.* **2016**, *19*, 914–922. [CrossRef]

24. Pathak, P.D.; Mandavgane, S.A.; Kulkarni, B.D. Fruit peel waste: Characterization and its potential uses. *Curr. Sci.* **2017**, *113*, 444–454. [CrossRef]